

Parameters of the X-ray binary system Scorpius X-1

A. M. Cherepashchuk,[★] T. S. Khruzina[★] and A. I. Bogomazov^{✉★}

M. V. Lomonosov Moscow State University, P. K. Sternberg Astronomical Institute, Universitetkij prospect 13, 119234 Moscow, Russia

Accepted 2021 September 1. Received 2021 August 27; in original form 2021 February 8

ABSTRACT

We modelled optical light curves of Sco X-1 obtained by the *Kepler Space Telescope* during the *K2* mission. Modelling was performed for the case of strong heating of the optical star and accretion disc by X-rays. In the model considered, the optical star fully filled its Roche lobe. We investigated the inverse problem in wide ranges of values of model parameters and estimated the following parameters of Sco X-1: the mass ratio of components $q = M_x/M_v = 3.6$ (3.5–3.8), where M_x and M_v are the masses of the neutron and optical stars correspondingly; the orbital inclination was $i = 30^\circ$ (25–34°). In the brackets the uncertainties of parameters q and i are shown; these originated due to uncertainties of characteristics of the physical model of Sco X-1. The temperature of the non-heated optical star was $T_2 = 2500$ –3050 K, its radius was $R_2 = 1.25R_\odot = 8.7 \times 10^{10}$ cm, and its bolometric luminosity was $L_{\text{bol}} = (2.1$ –4.6) $\times 10^{32}$ erg s⁻¹. The mass of the star was $M_v \simeq 0.4 M_\odot$. The contribution of the X-ray-heated accretion disc dominated in the total optical emission of Sco X-1. The transition between low and high states occurred due to the increase of X-ray luminosity by a factor of 2–3.

Key words: binaries: close – stars: neutron – stars: individual: Sco X-1 – accretion – accretion discs.

1 INTRODUCTION

The persistent low-mass X-ray binary system Sco X-1 = V818 Sco was the first compact X-ray source found outside the Solar system (Giacconi et al. 1962). A model of an X-ray binary with a neutron star (NS) for Sco X-1 was suggested by Shklovskii (1968), but final approval of this model was given later (Gottlieb, Wright & Liller 1975; Cowley & Crampton 1975). The cause of the delay was the high irregular variability of the object V818 Sco ($B = 11.1$ –14.1 mag; see e.g. Sandage et al. 1966; Hiltner & Mook 1967, 1970; Bradt et al. 1975; Canizares et al. 1975; Mook et al. 1975), and it was very difficult to find any periodicity in the brightness changes and spectra of this source. Numerous studies of Sco X-1 in the X-ray, optical, and radio ranges (see e.g. the catalogue by Cherepashchuk et al. 1996) made it possible to understand the main features of this system of the Z-source subclass (Hasinger & van der Klis 1989), the subclass of bright X-ray sources of the bulge. In the X-ray diagram ‘colour in the soft range – colour in the hard range’ (Hasinger & van der Klis 1989) the corresponding locus was similar to the letter ‘Z’ with three branches: a horizontal branch (HB), a normal branch (NB), and a flaring branch (FB).

As a typical Z-source Sco X-1 showed X-ray flux in the lower part of the Z-diagram close to the Eddington limit; this fact was used to estimate the distance to Sco X-1 as $d = 2 \pm 0.5$ kpc, and the corresponding colour excess was $E(B - V) \simeq 0.30$ mag (see e.g. Cherepashchuk et al. 1996). Sco X-1 showed quasi-periodical oscillations of the X-ray radiation with frequencies of about 6.3 Hz in NB, about 14.4 Hz in the lower part of FB, and about 10–20 Hz in HB.

Herewith the accretion rate on the NS monotonically grew along the Z-shaped curve in the diagram of X-ray colours from $0.4 \times 10^{-8} M_\odot \text{ yr}^{-1}$ in HB and $0.6 \times 10^{-8} M_\odot \text{ yr}^{-1}$ in NB up to $1.1 \times 10^{-8} M_\odot \text{ yr}^{-1}$ in FB (Vrtilek et al. 1991). There are also alternative interpretations of Z-diagrams where the accretion rate does not increase monotonically (see e.g. Church et al. 2012). It is generally accepted that Z-sources have higher accretion rates in comparison with numerous atoll (‘island’) sources with sub-Eddington accretion.

The optical variability of Sco X-1 showed bimodal and even trimodal character (see e.g. Bradt et al. 1975; Canizares et al. 1975; Mook et al. 1975). Around the lowest optical flux the optical variability was anticorrelated with the X-ray flux; during the brightening of Sco X-1 there was a correlation of the optical flux with the X-ray flux variability within the FB branch of the Z-diagram (see e.g. Ilovaisky et al. 1980; Petro et al. 1981; Augusteijn et al. 1992; McNamara et al. 2003; McGowan et al. 2003). An analysis of the correlation between the X-ray and optical variabilities of Sco X-1 and estimates of characteristic delay times of the optical variability in comparison to the X-ray variability ($\Delta t \simeq 10 \pm 5$ s) was performed by Muñoz-Darias et al. (2007), Britt (2013). The correlation between the optical and X-ray variabilities was observed only if Sco X-1 was in the bright X-ray state and was located in the FB branch of the X-ray Z-diagram. A regular optical variability of Sco X-1 with a period ≈ 18.9 h was discovered using archival photographic plates by Gottlieb et al. (1975) and was confirmed using spectroscopic observations (Cowley & Crampton 1975).

Scaringi et al. (2015), Hakala et al. (2015), Hynes et al. (2016) conducted an analysis of optical observations of Sco X-1 obtained by the *Kepler K2* mission and X-ray observations obtained by *Fermi* GBM and MAXI. The average wavelength of wide wavelength range observations of the *Kepler K2* mission was in the middle of a band

* E-mail: cherepashchuk@gmail.com (AMC); kts@sai.msu.ru (TSK); a78b@yandex.ru (AIB)

that corresponded to the *B*, *V*, *R* filters. Optical observations of Sco X-1 by *Kepler* in its *K2* programme were performed for 78.8 d in 2014 August–November. The exposure time for an individual observation was 54.2 s. Hynes et al. (2016) made careful analysis of the random and systematic errors of the *Kepler K2* observations and extracted 115 680 individual measurements for Sco X-1. These data allowed the construction of a light curve of this object with 1 per cent precision. Using the standard sinusoidal light curve, Hynes et al. (2016) independently found the photometric period of Sco X-1 to be $P = 0.78747 \pm 0.00072$ d, which is in good agreement (within error) with the more exact spectroscopic period $P = 0.7873114 \pm 0.000005$ d measured using the Doppler shift of the narrow emission Bowen lines N III/C III (Galloway et al. 2014).

Folding of all optical *Kepler K2* observations on the spectroscopic period showed that the average modulation of Sco X-1 brightness was one wave during one orbital period (the ‘reflection effect’; see Cherepashchuk et al. 1972; Lyutyi, Syunyaev & Cherepashchuk 1973) and could be clearly split in two states: high and low (Hynes et al. 2016). The amplitudes of the regular orbital optical light curves obtained by *Kepler K2* in the high and low states (in the supposition of sinusoidal variability) were practically the same at ≈ 0.15 mag. The difference between the average values of Sco X-1 brightness in the high and low states (in the same supposition) reached ≈ 0.4 mag.

After removal of the orbital trend from individual observations, Hynes et al. (2016) concluded that in the low state the system showed mostly bright optical flashes with duration $\Delta t \leq 1$ d, whereas in the high state there were fast ($\Delta t = 8$ –16 min) flashes and slow ($\Delta t = 2$ –5 d) dips. Hynes et al. (2016) presented average optical light curves of Sco X-1 in the high and low states (and an average overall light curve obtained by the *K2* mission) and qualitatively analysed them using sinusoidal fits of observed light curves.

It was very interesting to make detailed models of these very valuable observational data about Sco X-1 using modern mathematical descriptions of interacting binary systems (Khruzina et al. 2001, 2003a, b, 2005, 2015; Bisikalo 2005; Lukin et al. 2017; Cherepashchuk et al. 2019a, b).

2 OPTICAL LIGHT CURVES (ORBITAL)

Hynes et al. (2016) obtained the average light curves of Sco X-1 in white light using *Kepler K2* data; they also used spectroscopic data by Galloway et al. (2014): the epoch of the lower conjunction of the optical star $T_0 = \text{HJD } 2454635.3683 \pm 0.0012$, the spectroscopic orbital period $P = 0.7873114 \pm 0.000005$ d, the semi-amplitude of the radial velocity curve of the optical star (obtained using Doppler shifts of narrow Bowen emission lines N III/C III) $K = 74.9 \pm 0.5$ km s⁻¹.

Hynes et al. (2016) conducted a qualitative analysis of the shape and amplitude of orbital light curves in low and high states and on average. It was noted that all three curves were quasi-sinusoidal; there were no significant differences between amplitudes in high and low states (the full amplitude was 0.147 ± 0.012 mag in the low state and 0.151 ± 0.008 mag in the high state). It was possible to suspect a small phase shift to lower phases for the low state ($\Delta\varphi = 0.032 \pm 0.024$ in units of the orbital period), but this shift was at the 2σ level so it seemed insignificant. Hynes et al. (2016) also made a careful analysis of the influence of random and systematic deviations on the shape of the orbital light curves.

For further analysis we digitized data from fig. 3 by Hynes et al. (2016) using a special computer program. Hynes et al. (2016) presented optical light curves of Sco X-1 as the linear dependence of the quantity of counts of the photodetector $N(t)$ on time t . To convert the number of counts to stellar magnitudes we used the average

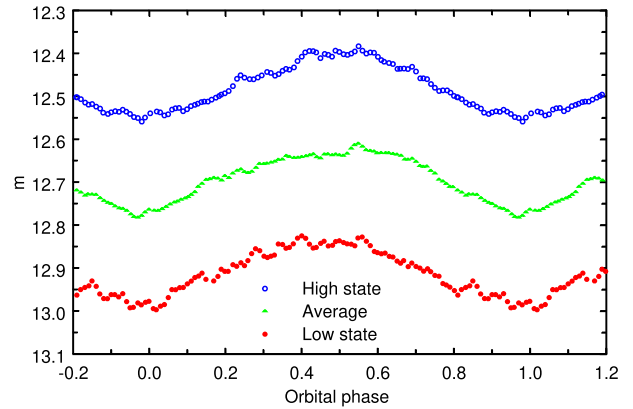


Figure 1. Light curves of Sco X-1 in low and high states (and an average curve) in stellar magnitudes calculated using equation (1).

quantity of counts (130 000 counts s⁻¹), which was close to the average state of the system (Hynes et al. 2016). Using photometric data by Galloway et al. (2014) obtained in 2001–2009 we were able to attribute the stellar magnitude $V = 12.7$ mag to the average value 130 000 counts s⁻¹. For the period of *K2* observations the AAVSO catalogue¹ contained data about Sco X-1 between 2014 August 1 and October 11 (which partially covered *Kepler*’s observations). The optical brightness *V* was in the range 12.0–13.233 mag, the average value between the maximum and minimum of these values was 12.62 mag, and the average value of all available 58 points in this period of time was 12.34 mag. Both quantities were close to our assumption ($V = 12.7$ mag). Moreover, since for our calculations relative changes in the light curves were important, the result weakly depended on the absolute calibration of the light curves. After recalculation of the linear-count scale to the stellar-magnitude scale using

$$m = 12.7 - 2.5 \log \left(\frac{N}{130\,000} \right), \quad (1)$$

we obtained orbital light curves of Sco X-1 in stellar magnitudes. They can be found in Fig. 1.

3 MATHEMATICAL MODEL OF THE SYSTEM

To interpret the light curves we used a model of an interacting binary system that took into account the results of three-dimensional gas-dynamic calculations (Bisikalo 2005; Lukin et al. 2017). In this model the region of the interaction of the gas stream with the outer border of the accretion disc was a combination of a hot line oriented along the gas stream and a hotspot within the outer border of the accretion disc. A detailed description of this model was given by Khruzina (2011) and applications of the model to cataclysmic and X-ray binaries were described by Khruzina et al. (2001, 2003a, b, 2005, 2015) and Cherepashchuk et al. (2019a, b).

In Sco X-1 there is a strong X-ray heating effect $L_x^{\text{max}}/L_{\text{opt}} \approx 500$, so the role of gas-dynamic interactions of the stream and disc is insignificant in comparison with it. Therefore, despite the fact that the model in its general form contains around 16 free parameters (which could be found if the system had eclipses), we used a mathematical model with six free parameters.

¹<https://www.aavso.org/>

In our mathematical model we used the standard method of synthesis of light curves of close binary systems by Wilson & Devinney (1971). The optical donor star filled its Roche lobe. The model took into account the linear limb darkening and gravitational darkening ($\beta = 0.08$, $T \sim g^\beta$, where g is the free-fall acceleration at the star's surface, Lucy 1967); it also took into account the heating of the surface of the star and accretion disc by X-ray radiation. Fluxes from elementary areas on the star's surface, on the accretion disc, and within the interaction region between the gas stream and the disc were calculated using Planck's law with corresponding local temperatures.

Due to the strong X-ray heating in the Sco X-1 system the temperature of the non-disturbed (non-heated) optical star T_2 cannot be set a priori but should be found in the course of the inverse problem solution. The mass ratio $q = M_x/M_v$ (M_x, M_v are the masses of the relativistic object and the optical star correspondingly) also cannot be fixed, because, in particular, the correction of the orbital radial velocity curve (which can take into account the asymmetric position of the place of origin of Bowen lines) strongly depended on the model (Muñoz-Darias, Casares & Martínez-Pais 2005; Galloway et al. 2014; Hynes et al. 2016). It should be noted that in the case of strong X-ray heating the task of optical light-curve interpretation became sensitive to changes of q , because q depends on the radius of the donor star (i.e. on the part of the X-ray flux that falls on the star).

The leading role in interpretations of orbital light curves of Sco X-1 belonged to the account of the 'reflection effect' and conversion of the energy of the central source in the accretion disc.

The X-ray heating for the optical star was considered in the assumption of an extended central X-ray source irradiating the star isotropically. The temperature of every elemental area on the heated part of the optical star was calculated as the sum of the bolometric flux from the non-disturbed star and of the bolometric flux from the X-ray source:

$$\sigma T^4 = \sigma T_0^4 + (1 - \eta_s) F_x^{\text{bol}}, \quad (2)$$

where T is the resulting temperature of the area, F_x^{bol} is the falling bolometric flux, T_0 is the temperature of the non-disturbed area on the star, σ is the Stefan–Boltzmann constant, and η_s is the albedo of the optical star that does not exceed 0.5 according to de Jong, van Paradijs & Augusteijn (1996).

To calculate the X-ray heating of the accretion disc we also used the model of an extended central source as a sphere with a small radius R_1 and with a surface temperature T_{in} . The parameters R_1 and T_{in} are included in the temperature distribution on the non-disturbed accretion disc:

$$T(r) = T_{\text{in}} \left(\frac{R_1}{r} \right)^{\alpha_g}, \quad (3)$$

where $\alpha_g \leq 0.75$ (Shakura & Sunyaev 1973). Parameters R_1 and T_{in} were free task parameters of our model. A quasi-parabolic surface of the accretion disc was heated by the slanting X-rays emitted by this sphere. In our model the heating was calculated as the sum of the bolometric flux from the non-disturbed disc (this flux was determined by the gravitational energy release during the accretion) and from the central sphere. In doing so we used a formula that was an analogue of equation (2), where the disc's albedo was taken to be equal to $\eta_d = 0$ and $\eta_d = 0.9$. As was shown by de Jong et al. (1996), only a small part of the X-ray radiation can be reprocessed to the optical range during the X-ray heating of the disc by the slanting X-ray radiation, so $(1 - \eta_d) \simeq 0.1$.

The basis of the model of the small extended central X-ray source for X-ray heating was found by Dubus et al. (1999), who noted that a

point X-ray source should be shielded by the accretion disc's body; in order to provide significant X-ray heating of the outer part of the disc the central source should be outside the disc's plane or the disc should be distorted. We accept the symmetric non-distorted disc; the X-ray heating was calculated in the model of a small extended X-ray source that can be thicker than the inner part of the accretion disc. Also there was a theoretical consideration in favour of the extended central source model (Bisnovatyi-Kogan & Blinnikov 1977; Mitsuda et al. 1984; White, Peacock & Taylor 1985): the X-ray radiation during accretion on the neutron star underwent significant Compton scattering in the corona of the accretion disc.

It was essential to identify a detailed spectrum of X-ray radiation (irradiating the donor star and the accretion disc) to calculate the 'reflection effect' in lines (Antokhina, Cherepashchuk & Shimanskii 2005). The presence of the soft component in the X-ray spectrum of the accreting relativistic object led to the formation of emission lines in profiles of absorption lines of the optical star. In addition, the strong X-ray heating of the optical star can lead to a significant outflow of matter in the form of an induced stellar wind from the heated part of the star (Basko & Sunyaev 1973). Narrow emission lines (caused by the Bowen mechanism) were able to form around the starting point of this wind. The wind can also be emitted from the highly heated accretion disc.

In our case we had orbital light curves of Sco X-1 in a wide range optical continuum. To calculate the 'reflection effect' we needed only the bolometric luminosity of the source (which strongly changed with time, $L_X = (0.6-12) \times 10^{37}$ erg s⁻¹, Cherepashchuk et al. 1996) as a first approximation. Therefore we limited ourselves by a simple fit of the X-ray source using Planck's law and the average temperature that can be estimated using the observed X-ray luminosity L_X . An approximate calculation of the temperature should be performed using the formula $L_X = 4\pi\sigma T^4 R_{\text{NS}}^2$, where $R_{\text{NS}} \approx 10-20$ km is the neutron star's radius. The value of T in this case was $(3-5) \times 10^7$ K. However, the size of the elementary areas on the surface of the central sphere in our mathematical model of Sco X-1 was approximately 1000 times greater than the size of the neutron star, so we were forced to average the temperature over surfaces with sizes $\sim 10^3 R_{\text{NS}}$; the bolometric X-ray luminosity L_X remained unchanged in this operation. Therefore the average temperature within the sphere's surface dropped to $T_{\text{in}} \sim 10^6$ K, and the model spectrum of X-ray radiation became significantly softer in comparison with the observed spectrum. Nevertheless, calculations of the 'reflection effect' in continuum required only the bolometric X-ray luminosity of the source, so the described approximation was taken as satisfactory. It allowed us to easily parametrize the effectiveness of the X-ray heating of the optical star and of the accretion disc using several parameters. These were T_{in} and R_1 in equation (3); others were the disc's opening angle β_d at its outer border (which characterized the size of the shadow from the X-ray source on the surface of the optical star) and the disc's albedo η_d .

We modelled three optical light curves of Sco X-1 for the low state, the high state, and the average curve (see Fig. 1). Transitions between low and high states can be associated either with the change of the intrinsic luminosity of the X-ray source (which in our case followed from the change of temperature T_{in}), with the shielding of the X-ray radiation of the central source by gas-stream structures situated close to the accretion disc, or with the change of the irradiation efficiency due to the variable shape of the distorted accretion disc (Dubus et al. 1999). We explained transitions between states by the change of the temperature of the central sphere T_{in} .

The value of T_{in} in the low state of Sco X-1 was noted as T_1 . To solve the inverse problem we started with the grid of T_1 values

and from the solution of the interpretation of the light curve in the low state we found corresponding values of R_1 along with other model parameters. The grid of bolometric luminosity values $L_{\text{bol}}^i = 4\pi R^2 \sigma (T_1^i)^4$ was calculated, then the value of T_1 (which corresponds to the X-ray luminosity in the low state) was found.

The X-ray luminosity in the Sco X-1 system greatly changed from one epoch to another; therefore we interpreted orbital optical light curves for a wide range of values of the parameter $T_1 = 10^5$ – 10^7 K.

If T_1 was $> 10^6$ K the bolometric luminosity of the central part of the accretion disc became $L_{\text{bol}}^c > 10^{38}$ erg s $^{-1}$ and it was greater than the Eddington limit for the neutron star. Nevertheless, for methodological reasons we used values greater than 10^{38} erg s $^{-1}$ to trace the changes of parameters in our inverse problem when the X-ray heating was changed in the wide range.

In the general case, for a given value of T_1 in our inverse problem (as already mentioned above), there were 16 free parameters. However, due to the strong X-ray heating in Sco X-1 it was possible to limit the quantity of free parameters to six: q , i , T_2 , T_{in} , R_1/a_0 , and R_d/a_0 , where T_{in} and R_1 are parameters of the central sphere (see equation 3), a_0 is the radius of the system's relative orbit, R_d/a_0 is the radius of the accretion disc in units of the radius of the orbit, and T_2 is the temperature of the non-disturbed optical star.

To solve the inverse problem the Nelder–Mead method was used; we minimized the functional Δ of the weighted sum of squares of residuals between observed and theoretical curves (Himmelblau 1972).

The solution of the inverse problem was performed by variations in one essential parameter. The value of q was fixed and the minimization of the functional of residuals was done; then the value of q was changed again and the minimization procedure was repeated. As the output of this process the dependence of the minimum of residuals Δ_{min} on the parameter q was calculated. Using this minimum of residuals the optimal value of q was found. The same procedure was conducted to find the optimal value of the orbital inclination i . To avoid getting to a local minimum of the functional of residuals we took a lot (several tens) of initial values for the free parameters.

As pointed out earlier, to interpret the light curve in the low state, T_1 was accepted to be equal to T_{in} , and the minimization of the functional of residuals was performed over the five remaining parameters. Finally, optimal values of q , i , R_1 , T_2 , and R_d for the low state were found, corresponding to $T_1 = T_{\text{in}}$.

For the average light curve and the light curve in the high state, T_1 was used in the form of the initial approximation and was accepted as the low limit for T_{in} . As a result of the minimization of the functional of residuals, values of six free parameters were found: q , i , R_1 , T_{in} , T_2 , R_d .

At the same time the value of T_{in} significantly changed in the transition between low and high states; therefore the bolometric luminosity L_{bol}^c of central parts of the disc (which provided the X-ray heating of the star and disc) also changed. This luminosity L_{bol}^c can become comparable to the observed X-ray luminosity L_X of the Sco X-1 system (which can change from one epoch to another in the range 6×10^{36} – 1.2×10^{38} erg s $^{-1}$).

4 RESULTS OF MODELLING

We performed modelling for a wide range of the parameter T_1 equal to 10^5 , 5×10^5 , 10^6 , 2×10^6 , and 10^7 K. Because of a significant lack of knowledge of specific values of the X-ray albedo of the star η_s and disc η_d along with the lack of precise knowledge of the disc's opening angle β_d we considered at first the simplest case

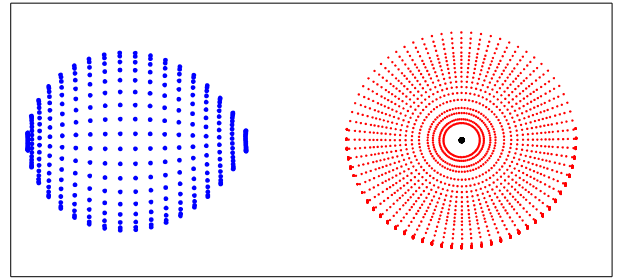


Figure 2. A computer model of the system calculated using optimal values of the free parameters; the optical star fully filled its Roche lobe ($\mu = 1$). The following parameter values were used: $T_1 = 10^6$ K, $q = 3.5$, $i = 20^\circ$, $R_d = 0.344a_0 = 0.56\xi$. The hot line and the hotspot are not shown, because their contributions to the total flux are insignificant.

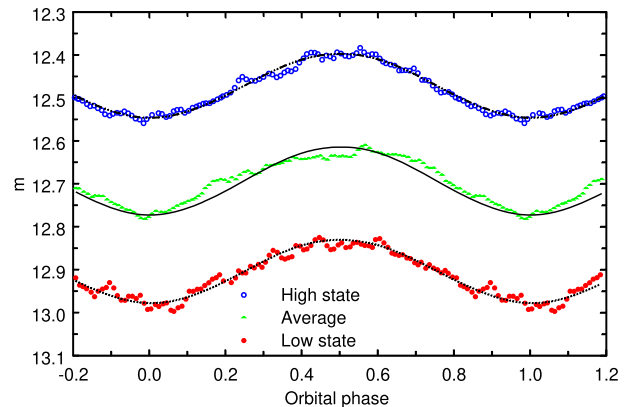


Figure 3. Observed light curves of Sco X-1 with superimposed optimal theoretical light curves (synthesized using parameters from Table 1, $T_1 = 10^6$ K, $\mu = 1$) in both states (low and high) and for the average curve.

$\eta_s = \eta_d = 0$, and for the opening angle we accepted the standard value from the theory of disc accretion (Shakura & Sunyaev 1973), $\beta_d = 3.2^\circ$.

4.1 X-ray luminosities close to observed values

First the interpretation of optical light curves of Sco X-1 was considered. Two values of T_1 were used (5×10^5 and 10^6 K), corresponding (for the R_1 values found below) to bolometric luminosities of the central source (in the disc) in the low state $L_{\text{bol}}^c = 3.3 \times 10^{36}$ erg s $^{-1}$ and $L_{\text{bol}}^c = 2.6 \times 10^{38}$ erg s $^{-1}$. These values were close to the minimum and maximum values of the observed X-ray luminosity of Sco X-1 ($L_X = 6 \times 10^{36}$ erg s $^{-1}$ and $L_X = 1.2 \times 10^{38}$ erg s $^{-1}$ correspondingly). A computer model of the system is shown in Fig. 2; this was computed using optimal values of the free parameters.

In Fig. 3 are shown observed light curves of Sco X-1 with superimposed optimal theoretical light curves in both states (low and high) and for the average curve. It can be seen that, despite the fact that observations and theory are in good agreement in general, in several parts there are discrepancies. This is due to complicated physical processes in the system that were not accounted for in our mathematical model. For normally distributed points in the light curve, minimum residuals Δ_{min} should be distributed by the law χ_{N-M}^2 , where N is the quantity of ‘normal’ points within the light curve and M the quantity of free parameters used for the minimization of residuals.

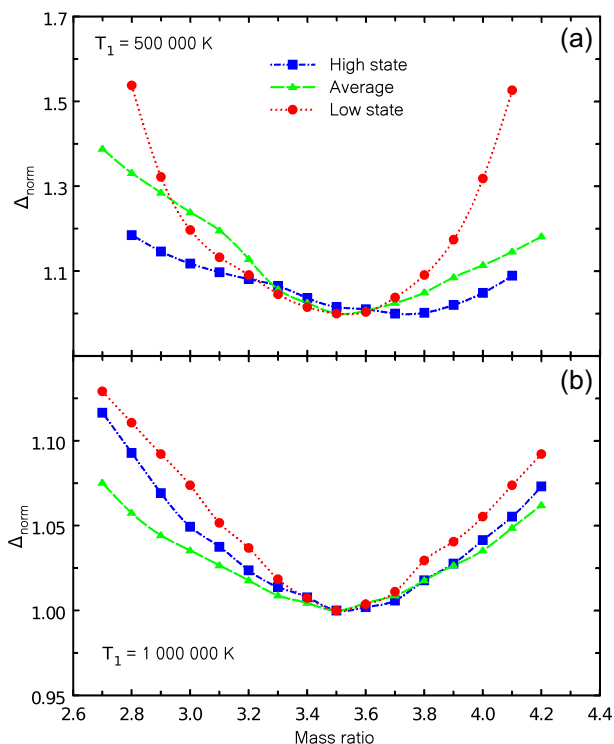


Figure 4. Dependences of relative residuals $\Delta_{\text{norm}} = \chi^2/\chi_{\text{min}}^2$ minimized over all parameters except the mass ratio q for $T_1 = 5 \times 10^5$ and 10^6 K.

As noted by Hynes et al. (2016) the application of standard statistical criteria based on χ^2 statistics cannot be entirely justified, because the observed points in the *Kepler K2* mission were potentially distributed non-normally. Nevertheless, we formally used the χ^2 criterion for clearer visualization of the results.

Calculations showed that the minimum residuals Δ_{min} corresponded to $\chi^2 = \frac{\Delta_{\text{min}}}{N-M} \gg 1$ (from 3–6). This fact indicates that our mathematical model was very simplified. Nevertheless, it was possible to choose optimal values of free parameters using minimum residuals Δ (if the sensitivity of the problem to changes of free parameters was sufficient). In this way we understood all the found parameter values of the model.

In Fig. 4 we show the dependence of residuals on the mass ratio q minimized over all parameters (except q). Residuals Δ_{norm} were normalized using the minimum value Δ_{min} among values computed for different q . Results are shown for two different values of the T_1 parameter ($T_1 = 5 \times 10^5$ and 10^6 K), in low and high states and for the average curve. It can be seen that all three curves demonstrate a significant dependence on the mass ratio. For $T_1 = 10^6$ K the value of q was $q = 3.5$; for $T_1 = 5 \times 10^5$ K it was the same. As noted above, since our model was incompletely adequate and the distribution of observational points of light curves was not normal, we show only optimal values of parameters q and i obtained by the minimum of residuals and we do not show their errors. It is remarkable that the optimal value of q does not depend (or depended only weakly) on the value of T_1 (i.e. on the X-ray heating). This can be easily understood: X-ray heating is mostly determined by the geometrical factor (by the relative dimensions of the donor star that filled its Roche lobe, the size of the lobe depending on q).

In Fig. 5 we show the dependence of residuals Δ_{norm} on the orbital inclination i (for $T_1 = 10^6$ and 5×10^5 K) minimized over all parameters (except i). Residuals are also shown for three variants

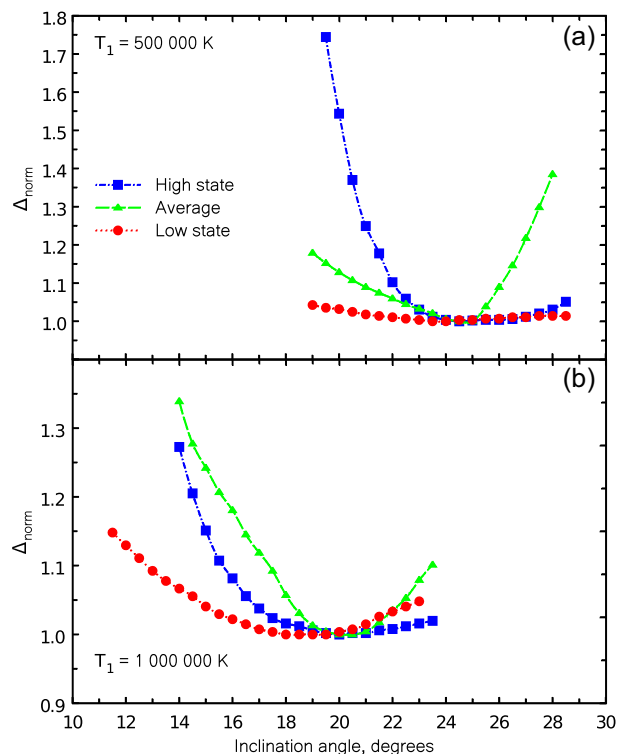


Figure 5. Dependences of relative residuals $\Delta_{\text{norm}} = \chi^2/\chi_{\text{min}}^2$ minimized over all parameters except the orbital inclination i for $T_1 = 5 \times 10^5$ and 10^6 K.

of the light curve. All curves are similar and show a significant dependence on i . For $T_1 = 10^6$ K the inclination was $i \approx 20^\circ$. For $T_1 = 5 \times 10^5$ K it was $i \approx 25^\circ$. It can be seen that (in contrast with the parameter q) the i parameter significantly depends on T_1 (i.e. on the X-ray heating). This is natural: if the value of X-ray heating increases, the difference between the average temperatures of the heated and non-heated parts of the donor star (with a fixed value of i) also increases, leading to an increase in the ‘reflection effect’. We do not give errors for q and i , because our mathematical model was not completely adequate to observations.

In Table 1 we show optimal values of Sco X-1 parameters calculated for $T_1 = 10^6$ K. It can be seen that the temperature of the non-heated part of the donor star was $T_2 = 3050$ K, corresponding to spectral type M4–M5 (Habets & Heintze 1981). The average radius of the optical star was close to $0.286a_0$, where a_0 is the radius of the relative orbit, which can be estimated using Kepler’s third law. Assuming the mass of the neutron star to be equal to its standard value $1.4M_\odot$, the mass of the donor star was found to be $0.4M_\odot$ for $q = 3.5$. For the total mass of both components $1.8M_\odot$ and for the orbital period 0.787 d the radius of the relative orbit was $a_0 = 4.37R_\odot$ and the absolute average radius of the donor star $R_2 = 1.25R_\odot = 8.7 \times 10^{10}$ cm. The bolometric luminosity of the donor star was $L_2 = 0.114L_\odot$ for the temperature $T_2 = 3000$ K. So, the donor star in Sco X-1 possessed a significant excess of the radius and luminosity; i.e. the star noticeably moved forward in its nuclear evolution. Since the nuclear time-scale for a $0.4M_\odot$ main-sequence star should be much longer than the current age of the Universe, it was necessary to suppose that the initial mass of the donor star was $> 0.8M_\odot$. The decrease of the donor star’s mass could happen due to a strong stellar wind stimulated by X-ray heating (Basko & Sunyaev 1973; Iben, Tutukov & Yungelson

Table 1. Optimal values of parameters of Sco X-1, obtained from the modelling of optical light curves of the *Kepler K2* mission for low and high states and for the average curve, $T_1 = 10^6$ K. T_2 is the effective temperature of the donor star, $\langle T_{\text{warm}} \rangle$ is the average temperature of this star on the heated part, R_d is the radius of the disc in units of ξ and a_0 , T_{in} is the average temperature of the disc's matter within the sphere with the R_1 radius, T_{out} is the same on the outer border, and α_g is the parameter that determines the temperature distribution along the disc's radius according to equation (3).

Parameters	Low state	Average	High state
T_2 , K	3050	3050	3050
$\langle T_{\text{warm}} \rangle$, K	20 715	24 700	27 565
R_d , ξ	0.535	0.555	0.606
R_d , a_0	0.332	0.344	0.376
T_{in} , K	1000 000	1204 310	1351 235
T_{out} , K	25 600	28 815	28 460
α_g , fixed	0.75	0.75	0.75
χ^2	292	329	503

Note. Parameters of synthetic light curves were obtained using following fixed values of the parameters (calculated in previous stages of this work): the mass ratio is $q = M_x/M_v = 3.5$, the orbital inclination is $i = 20^\circ$, the average radius of the donor star is $\langle R_2 \rangle = 0.286a_0$, the disc's eccentricity is $e = 0.01$, the argument of pericentre of the disc is $\alpha_e = 110^\circ$, the distance between the inner Lagrange point L1 and the centre of masses of the neutron star is $\xi = 0.6255a_0$, the radius of the central sphere in the disc is $R_1 = 0.003 14\xi = 0.001 96a_0$, $T_1 = 10^6$ K is the temperature of the matter around the R_1 distance in the low state, the thickness of the outer border of the disc is $\beta_d = 3.2^\circ$, and it is assumed that the flux in arbitrary units $F_{12.7} = 2.4558 \times 10^{-8}$ corresponds to the stellar magnitude in white light, 12.7 mag.

1995). Another possibility for the donor-star evolution is associated with its deviation from thermal equilibrium due to a relatively high mass-loss rate. The characteristic time of mass-loss by the star can become shorter than the time of thermal relaxation; as a result of this deviation the star should increase its radius, possessing a weakly evolved core (see e.g. Knigge 2006). The accretion disc's radius on average was $R_d = (0.54-0.61)\xi = (0.33-0.38)a_0$ for $T_1 = 10^6$ K, where $\xi = 0.626a_0$ is the distance between the disc's centre and the inner Lagrange point L1 and a_0 is the radius of the relative orbit. In the low state $R_d = 0.54\xi$, in the high state $R_d = 0.61\xi$; these values coincide within error. The temperatures T_{in} of the inner part of the accretion disc were 1.35×10^6 , 1.2×10^6 , and 10^6 K for the high state, the average curve, and the low state correspondingly. The obtained value of the radius of the radiating central part of the disc (the central sphere in our model) was $R_1/a_0 = 0.001 96$, i.e. $R_1 = 6 \times 10^8$ cm. The bolometric luminosities of the central part of the disc (which provide the X-ray heating of the star and disc) were $L_{\text{bol}}^c = 8.4 \times 10^{38}$, 5.3×10^{38} , and 2.5×10^{38} erg s $^{-1}$, respectively. These values were somewhat greater than the upper observed limit of the Sco X-1 X-ray luminosity ($L_X = 1.2 \times 10^{38}$ erg s $^{-1}$) and the Eddington limit for the neutron star. Nevertheless, in methodological terms the luminosity values clearly illustrate the cause of the transition from the low state to the high state: in the model of physical variability of the central X-ray source this happened due to the increase in the X-ray luminosity of the central part of the accretion disc by a factor of ≈ 3.36 . In our case the X-ray heating effect was observed in the optical range, i.e. in the Rayleigh-Jeans part of the spectrum. Therefore, during the transition between low and high states, the observed average optical brightness of the system should grow by a quantity that should be approximately proportional to the ratio of the corresponding inner temperatures. It should be several tens of per cent, and this estimate fits the observations. It is essential to note that the circumstances of donor-star irradiation

Table 2. The same as Table 1 for the temperature of the matter at the R_1 radius in the low state $T_1 = 5 \times 10^5$ K and the orbital inclination $i = 25^\circ$. The radius of the central sphere in the disc was $R_1 = 0.002 17\xi = 0.001 36a_0$.

Parameters	Low state	Average	High state
T_2 , K	2940	2940	2820
$\langle T_{\text{warm}} \rangle$, K	9260	10 550	11 230
R_d , ξ	0.636	0.637	0.685
R_d , a_0	0.394	0.395	0.424
T_{in} , K	500 000	580 000	623 880
T_{out} , K	10 890	11 500	11 700
α_g , fixed	0.713	0.710	0.702
χ^2	264	313	494

Note. The assumed stellar magnitude in white light is 12.7 mag; the flux that corresponds to this is $F_{12.7} = 7.283 \times 10^{-9}$ in arbitrary units.

can change because of a change in the accretion disc's thickness or because of variability in the anisotropy of the radiation of the central source.

In Table 2 we show the parameters of the system for $T_1 = 5 \times 10^5$ K. The temperature of the non-heated part of the donor star was 2800–2900 K. The average radius of the optical star was $\langle R_2 \rangle = 0.286a_0$. Since the radius of the optical star depends only on q , and $q = 3.5$ was the same for $T_1 = 5 \times 10^5$ and 10^6 K, the value of $\langle R_2 \rangle$ was also the same. The accretion disc's radius was $0.63-0.68\xi = (0.39-0.42)a_0$. The temperatures of the inner part of the disc T_{in} were 5×10^5 , 5.8×10^5 , and 6.2×10^5 K for the low state, the average curve, and the high state, respectively. The obtained radius of the radiating central part of the disc $R_1 = 0.001 36a_0 \approx 4.13 \times 10^8$ cm. The bolometric luminosities of the disc's central part (which provide the X-ray heating of the star and disc) were 1.9×10^{37} , 1.4×10^{37} , and 8×10^{36} erg s $^{-1}$ for the high state, the average curve, and for the low state, respectively. These values are close to the lower limit of the observed Sco X-1 X-ray luminosity ($L_X = 6 \times 10^{36}$ erg s $^{-1}$). In the model of variability of the temperature of the central source, the increase in the luminosity of the central part of the accretion disc in the transition between low and high states from $8 \times 10^{36}-1.9 \times 10^{37}$ erg s $^{-1}$ (i.e. by a factor of 2.38) led to the corresponding change in the average brightness of the system.

Figs 6(a)–(c) demonstrate the temperature distribution in the heated (by X-rays) part of the optical star. Distributions of the temperature are shown for $T_1 = 5 \times 10^5$ and 10^6 K for the low and high states and for the average curve.

The zone around the Lagrange L1 point $\pm 5^\circ$ is shadowed by the accretion disc. This zone corresponds to the angle φ between the orbital plane and the radius-vector from the star's centre of masses to the centre of the elementary area from $5-95^\circ$. For the greater X-ray luminosity of the compact source ($T_1 = 10^6$ K) and for the high state the temperature decreased from $\approx 70 000$ K around the L1 point to ≈ 3000 K in the vicinity of the terminator (the terminator divides the heated and non-heated parts of the star's surface). The temperature of around several tens of thousands of kelvins was favourable for the formation of narrow emission lines N III/C III excited by the Bowen mechanism in the starting point of the optical star's wind (the wind was induced by X-ray heating, Basko & Sunyaev 1973).

In the case of moderate X-ray heating ($T_1 = 5 \times 10^5$ K) in the high state the temperature on the heated part of the optical star decreased from $\approx 27 000$ K around the L1 point to ≈ 3000 K in the vicinity of the terminator. As a result of the inverse problem solution (interpretations of light curves of Sco X-1) we computed light curves

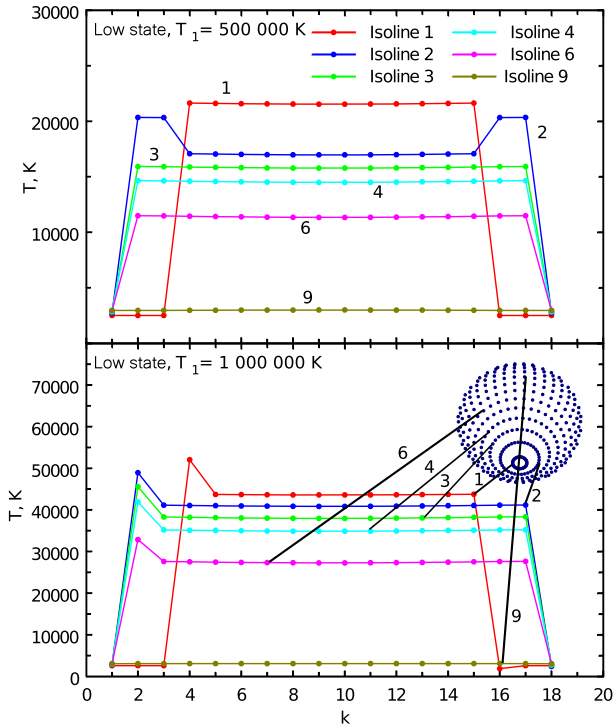


Figure 6. (a) The distribution of the temperature on the heated (by X-rays) part of the donor star over the orbital plane for the low state, $T_1 = 5 \times 10^5$ and 10^6 K. The region $\pm 5^\circ$ ($k = 1-2, 16-18$) around the L1 point ($j < 1$) is shadowed by the accretion disc (k is the index number of the area on the isoline j). This region corresponds to the angle φ between the orbital plane and the radius-vector from the star's centre of masses to the centre of the elementary area from 5° ($k = 1$) to 95° ($k = 18$). j shows the number of the isoline that was formed by elementary areas on the star. These areas with the same j have the same angle θ between the axis that connects the centres of the components and the mentioned radius-vector. $j = 1$ corresponds to $\theta = 5^\circ$, $j = 2$ to $\theta = 15^\circ$, and so on.

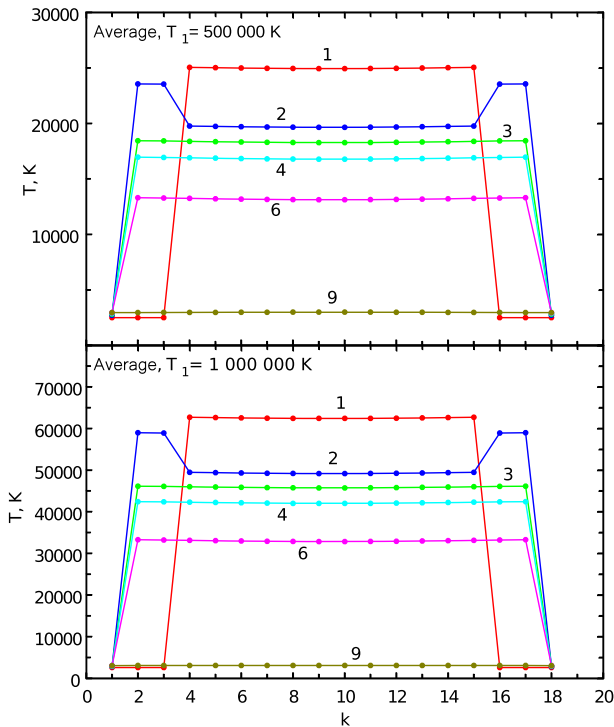


Figure 6. (b) The same as Fig. 6(a) for the average curve.

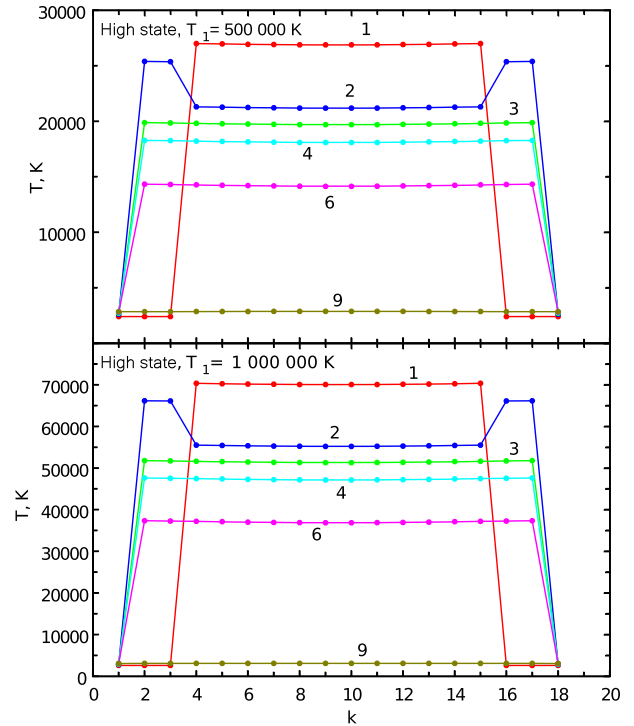


Figure 6. (c) The same as Fig. 6(a) for the high state.

for the entire system and for its components: for the donor star, the accretion disc, the hot line, and the hotspot (the contributions from the hot line and the hotspot were negligible; therefore they are not shown separately throughout this paper). These curves can be expressed in units of the average total luminosity of the system or in arbitrary absolute energetic units (a.e.u.). Arbitrary units can be converted to stellar magnitudes; in this case the flux of radiation for the corresponding T_1 should be found using the average brightness of Sco X-1 (12.7 mag; see above).

In Table 3 we show average luminosities of the disc and star during the orbital period in units of the total average luminosity of Sco X-1 and in arbitrary energetic units (a.e.u.), $T_1 = 10^6$ K. It can be seen that in both states and in the average curve the accretion disc's luminosity dominated. This luminosity decreased in the transition from the high state (≈ 0.83 a.e.u.) to the average curve (≈ 0.82 a.e.u.) and the low state (≈ 0.80 a.e.u.). On average the disc's luminosity was four to five times greater than the star's luminosity.

In Fig. 7 we show theoretical light curves of the star and disc for the low state. It can be seen that the disc's luminosity did not change with the phase of the orbital period (the contributions of the luminosities of the hotspot and the hot line were negligible). The average theoretical light curves of the star and disc and the curves for the high state and average light curve are qualitatively similar to the curves in Fig. 7.

The luminosities of the disc and star monotonically decreased in the transition between the low and high states. The light curve of the star itself was a single wave during the single orbital period (the 'reflection effect'; see e.g. Cherepashchuk et al. 1972; Lyutyi et al. 1973); the amplitude and average brightness of it increased in the transition between the low and high states.

The amplitude of observational light curves of Sco X-1 practically did not change (despite the fact that the average brightness of the system changed by 0.4 mag) due to the influence of the accretion

Table 3. Optical luminosities averaged for the orbital period (in the *C* band) of the disc and the stars of the system, expressed in units of the total average luminosity of Sco X-1 (Rel. flux) and in arbitrary absolute energetic units (a.e.u.), $T_1 = 10^6$ K, $i = 20^\circ$.

Component	Abs. flux, 10^{-8} a.e.u.	Rel. flux
Low state		
Optical star, F_2	0.32	0.159
Disc's central sphere, F_1	0.0022	0.0011
Disc, F_d	1.6320	0.7997
Total flux, F_{sys}	2.04026	1
Average		
Optical star, F_2	0.42	0.169
Disc's central sphere, F_1	0.0022	0.0009
Disc, F_d	2.02100	0.81580
Total flux, F_{sys}	2.47715	1
High state		
Optical star, F_2	0.49	0.160
Disc's central sphere, F_1	0.0022	0.0007
Disc, F_d	2.5070	0.82550
Total flux, F_{sys}	3.03677	1

Note. Contributions of the hot line and hotspot to the flux are insignificant; therefore they are not shown.

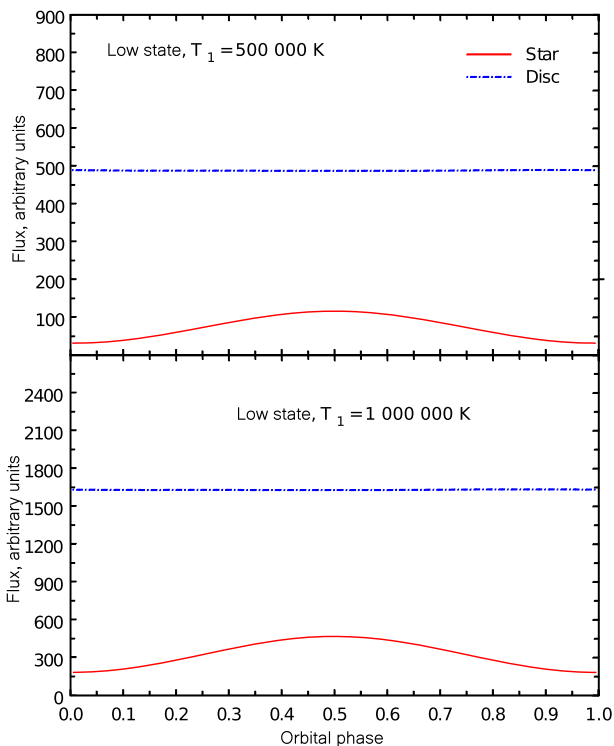


Figure 7. Light curves of the donor star and accretion disc calculated as the solution of the inverse problem; for the low state, T_1 was 5×10^5 and 10^6 K. The accretion disc dominated in the total optical luminosity in all considered cases.

disc's radiation and the value of the amplitude of the optical star's light curve and its average brightness.

In Table 4 we show average luminosities of the disc and star during the orbital period in units of the total average luminosity of Sco X-1 and in a.e.u., $T_1 = 5 \times 10^5$ K. It can be seen that the ratios of the luminosities of the star and disc are similar to the case of $T_1 = 10^6$ K.

Table 4. The same as Table 3 for $T_1 = 5 \times 10^5$ K, $i = 25^\circ$.

Component	Abs. flux, 10^{-8} a.e.u.	Rel. flux
Low state		
Optical star, F_2	0.74	0.122
Disc's central sphere, F_1	0.0050	0.0008
Disc, F_d	4.885	0.8086
Total flux, F_{sys}	6.04101	1
Average		
Optical star, F_2	0.98	0.134
Disc's central sphere, F_1	0.0050	0.0007
Disc, F_d	6.1820	0.84070
Total flux, F_{sys}	7.35423	1
High state		
Optical star, F_2	1.13	0.125
Disc's central sphere, F_1	0.0050	0.0006
Disc, F_d	7.802	0.86650
Total flux, F_{sys}	9.00446	1

As follows from Fig. 8, the ratios of the disc's and star's luminosities practically did not depend on the values of the free parameters; therefore the conclusion about the domination of the accretion disc's luminosity in the total optical luminosity of Sco X-1 is reliable.

4.2 Wide range of X-ray luminosities

The modelling of the Sco X-1 system in a wide range of luminosities of the X-ray source (much higher and much lower than the observed values) was of great methodological interest. Additionally we interpreted light curves for $T_1 = 10^5$, 2×10^6 , and 10^7 K; the system's luminosities in the low state were 1.9×10^{33} , 8×10^{39} , and 2×10^{43} erg s $^{-1}$. Values of X-ray luminosities significantly greater than 10^{38} erg s $^{-1}$ were physically unrealistic, because they were greater than the Eddington limit of a neutron star with mass $1.4 M_\odot$. Nevertheless, as noted above, we used them for methodological reasons.

Let us consider the results of modelling for the low X-ray luminosity (the X-ray luminosity L_{bol}^c of a sphere with R_1 radius, $L_{\text{bol}}^c = 1.9 \times 10^{33}$ erg s $^{-1}$ for $T_1 = 10^5$ K) that just slightly exceeded the bolometric luminosity of the donor star ($\approx 4.4 \times 10^{32}$ erg s $^{-1}$). Even in such a case the optimal mass ratio q remained close to 3.5 (see Fig. 9). However (see Fig. 10), the orbital inclination angle $i = 34^\circ$ was significantly greater than $i = 20^\circ$ (for $L_{\text{bol}}^c = (2.5\text{--}8.4) \times 10^{38}$ erg s $^{-1}$, $T_1 = 10^6$ K). The increase in the orbital inclination with decreasing X-ray heating can be easily understood. If the X-ray heating is low the ellipsoidal shape of the star also becomes important along with the 'reflection effect' (which provides two waves in one orbital cycle). This leads (in the same circumstances) to a decrease in the amplitude of the optical star's light curve; therefore it is necessary to increase i to describe the observed light curves.

Let us consider two variations of our modelling corresponding to very high X-ray luminosity, $(0.8\text{--}2.9) \times 10^{40}$ erg s $^{-1}$ ($T_1 = 2 \times 10^6$ K) and $(2.0\text{--}8.7) \times 10^{43}$ erg s $^{-1}$ ($T_1 = 10^7$ K). As can be seen from Fig. 9, the optimal mass ratio also remains the same for these very high X-ray luminosities: $q \approx 3.5$.

At the same time (as follows from Fig. 10) the orbital inclination can be found using the minimum of residuals: $i \approx 15.5^\circ$ for $T_1 = 2 \times 10^6$ K ($L_{\text{bol}}^c = 8 \times 10^{39}$ erg s $^{-1}$) and $i \approx 14.5^\circ$ for $T_1 = 10^7$ K ($L_{\text{bol}}^c = 2 \times 10^{43}$ erg s $^{-1}$). The temperatures of the non-heated parts of the optical star in all considered cases ($T_1 = 10^5$, 2×10^6 ,

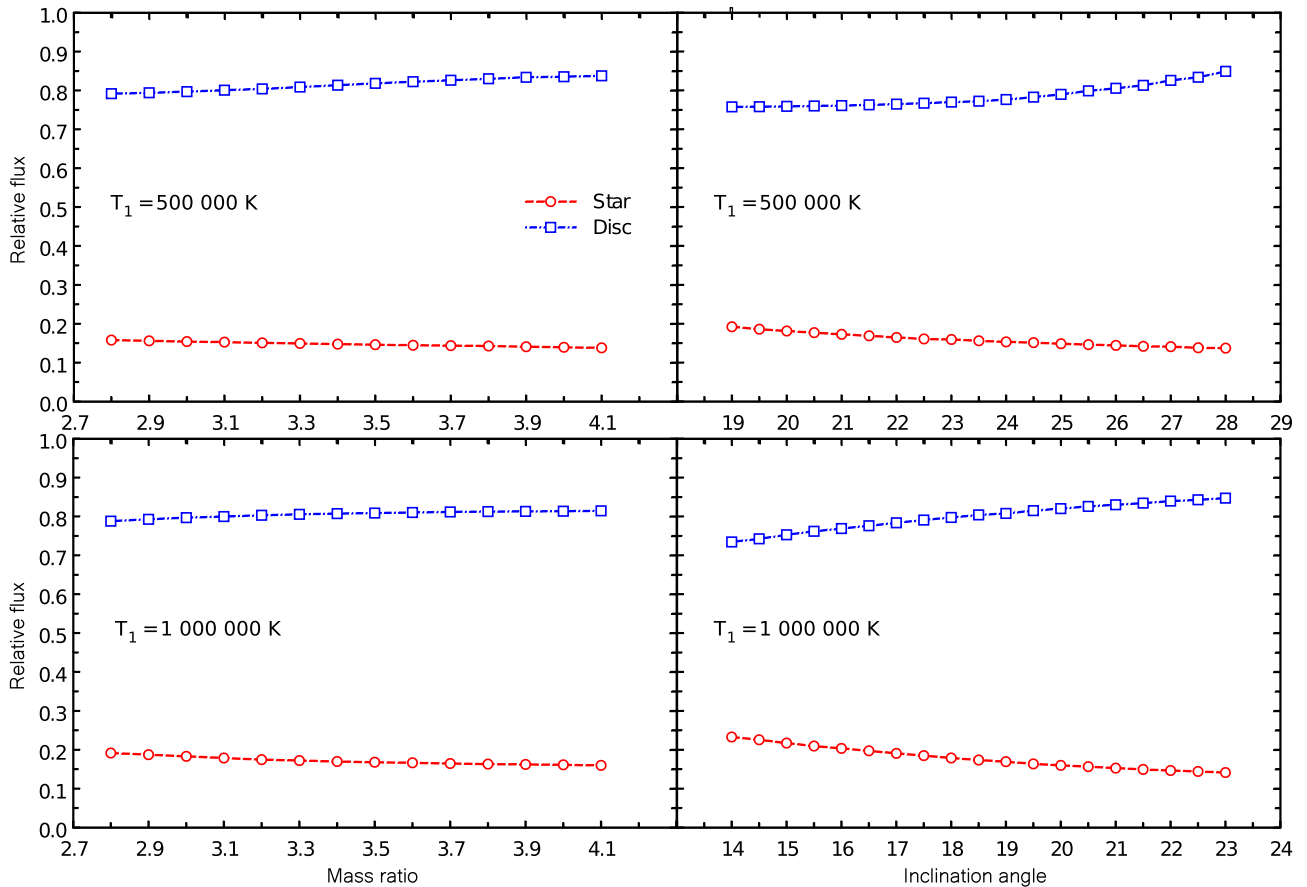


Figure 8. Dependences of relative (averaged over the orbital cycle) luminosities of the accretion disc and donor star on the parameters q and i for the average light curve, $T_1 = 5 \times 10^5$ and 10^6 K.

and 10^7 K) were close to 2500–3000 K. The temperatures of the heated parts of the star in the vicinity of the Lagrange point L1 were $\approx 1200\,000$, $\approx 140\,000$, and $\approx 3\,200$ K for $T_1 = 10^7$, 2×10^6 , and 10^5 K correspondingly (for the average light curve).

As follows from Fig. 11 in the cases of $T_1 = 10^5$, 2×10^6 , and 10^7 K, all regularities (found earlier) remain: the contribution of the accretion disc dominated in the total optical radiation of Sco X-1. Thus, this domination effect does not depend on parameters q , i and on the value of the system’s X-ray luminosity, because the solid angle of the accretion disc (which intercepted the X-ray radiation of the central source) was significantly greater than the solid angle of the optical star.

The most important results of our study are the estimates of parameters q and i . The value $q \simeq 3.5$ does not depend on the X-ray heating value and on the state of the system. At the same time the value of i weakly depends on the system’s state, but it strongly depends on the X-ray heating value.

In Table 5 and Fig. 12 we show the dependence of parameters i and q on the bolometric luminosity of the central part of the accretion disc in the low state (different values of T_1 are marked). The value $q \simeq 3.5$ remains the same for all values of the other parameters. The value of i monotonically decreases from $i = 34^\circ$ for $L_{\text{bol}}^c = 1.9 \times 10^{33}$ erg s^{-1} to $i = 14.5^\circ$ for $L_{\text{bol}}^c = 2 \times 10^{43}$ erg s^{-1} . In the range $L_{\text{bol}}^c = 8.0 \times 10^{36}$ – 2.5×10^{38} erg s^{-1} (which is close to the observed range of the X-ray luminosity of Sco X-1, $L_X = 6 \times 10^{36}$ – 1.2×10^{38} erg s^{-1}) the value of i is 25 – 20° .

5 THE INFLUENCE OF THE THICKNESS OF THE ACCRETION DISC AND OF ITS X-RAY ALBEDO ON THE LIGHT CURVE

5.1 The disc thickness

Since the accretion disc lies in the orbital plane it shields some of the X-ray flux leading to the presence of a shadow on the surface of the optical star. We conducted an analysis (see above) of optical light curves of Sco X-1 using the standard theory of disc accretion (Shakura & Sunyaev 1973). According to its predictions for the Sco X-1 parameters, the opening angle of the standard accretion disc should be $\beta_d = \pm 3.2^\circ$. This value (thickness) was used in the calculations above.

As was noted by de Jong et al. (1996), Dubus et al. (1999) the analysis of X-ray light curves of a number of low-mass X-ray binaries led to the conclusion that the real value of the opening angle can be up to 12 – 14° under the influence of X-ray heating. Such a high value of the disc’s opening angle can be theoretically explained (Meyer & Meyer-Hofmeister 1984): the thickness of the outer part of the disc should significantly grow if the X-ray heating is strong. Moreover, the X-ray heating of the accretion disc by the central X-ray source can distort the disc’s shape from symmetrical to curved (Pringle 1996; Maloney, Begelman & Pringle 1996; Maloney & Begelman 1997; Dubus et al. 1999).

Pringle (1996), Maloney et al. (1996), Maloney & Begelman (1997) showed that accretion discs irradiated by the central source

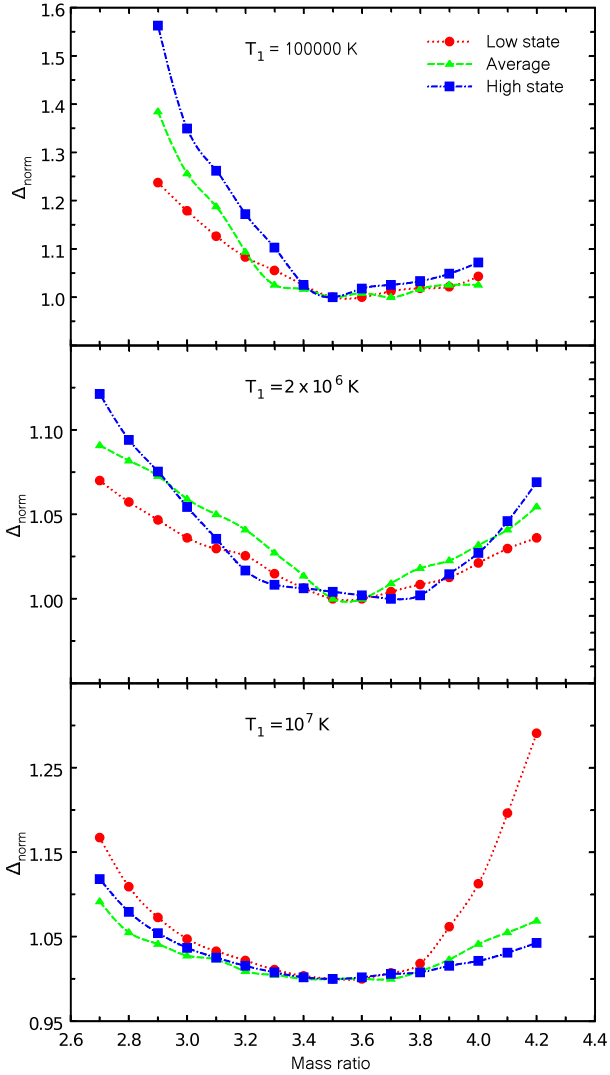


Figure 9. Dependences of relative residuals $\Delta_{\text{norm}} = \chi^2/\chi_{\text{min}}^2$ minimized over all parameters except the mass ratio q for $T_1 = 10^5$, 2×10^6 , and 10^7 K.

(an accreting relativistic object) should be unstable against bending. This can be explained by the non-axisymmetric radiation pressure (in the case of non-strictly flat discs) that can lead to disturbances in the disc and to disc bending. Such curved accretion discs can precess under the influence of the force from the optical star with a period much longer than the orbital period, as occurred in the Her X-1 X-ray binary.

The discovery of such long-period variability in Sco X-1 would be a strong argument in favour of the curved disc model. In this model the shadow on the heated surface of the optical star could be caused by shielding of the central X-ray source by the inner bent part of the accretion disc, but not by its outer part. Since such long-period ‘precessional’ variability was not found in Sco X-1, we considered a symmetric accretion disc with different opening angles ($\beta_d = 3.2$ – 14°).

An investigation into the influence of the opening angle on the results of our modelling was conducted for the average light curve of Sco X-1 using the value $T_1 = 5 \times 10^5$ K and three fixed values of β_d (3.2 , 10 , and 14°). In the first stage of calculations we assumed that the X-ray albedos of the optical star and accretion disc were $\eta_s = \eta_d = 0$. This was done to separately study the influence of parameters β_d ,

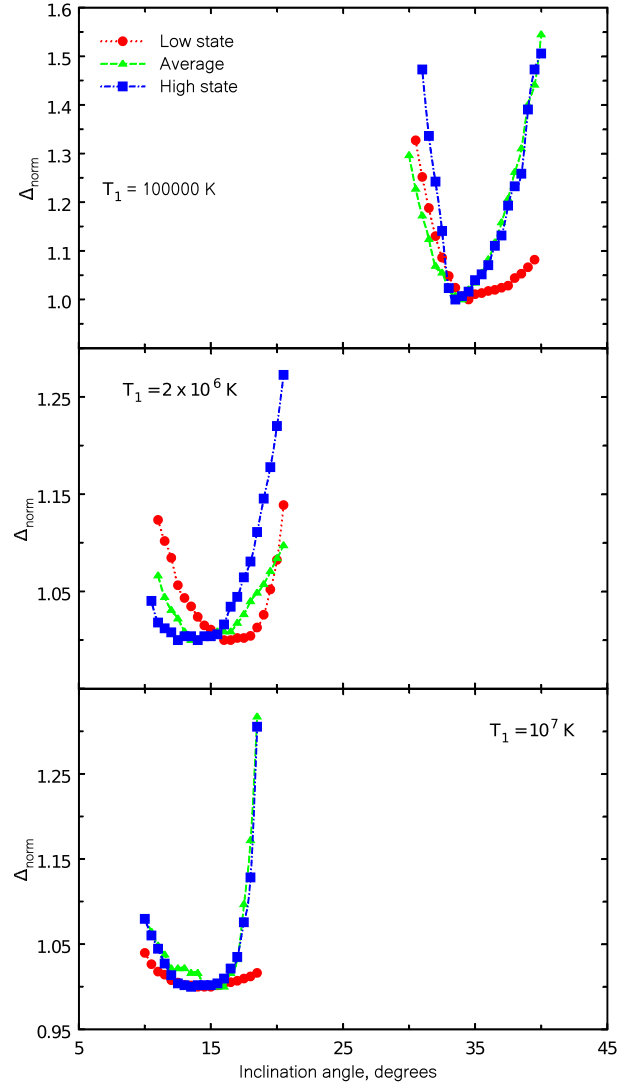


Figure 10. Dependences of relative residuals $\Delta_{\text{norm}} = \chi^2/\chi_{\text{min}}^2$ minimized over all parameters except the orbital inclination angle i for $T_1 = 10^5$, 2×10^6 , and 10^7 K.

η_s , and η_d on the results of the inverse problem solution. The method for the solution was the same.

In Fig. 13 we show the dependences of residuals between observed and theoretical light curves (normalized to minimal values) on parameters q and i ; the disc’s opening angle is marked by the quantities on the corresponding curves. It can be seen that the influence of the opening angle on the optimal value of the mass ratio $q = M_s/M_v$ is rather weak. The increase in β_d from 3.2 – 14° led to an increase in q from 3.5 – 3.8 . At the same time the change in the opening angle led to a significant change in the orbital inclination i ; for β_d values 3.2 , 10 , and 14° the values of i were 25 , 28 , and 34° correspondingly.

5.2 The X-ray albedo

de Jong et al. (1996) estimated values of η_s and η_d from the comparison of a model of the X-ray heating of the accretion disc with the observed X-ray luminosity of low-mass X-ray binary systems. They showed that the X-ray albedo of the donor star can be accepted as being equal to 0.5, and for the accretion disc it was 0.9 (i.e. only

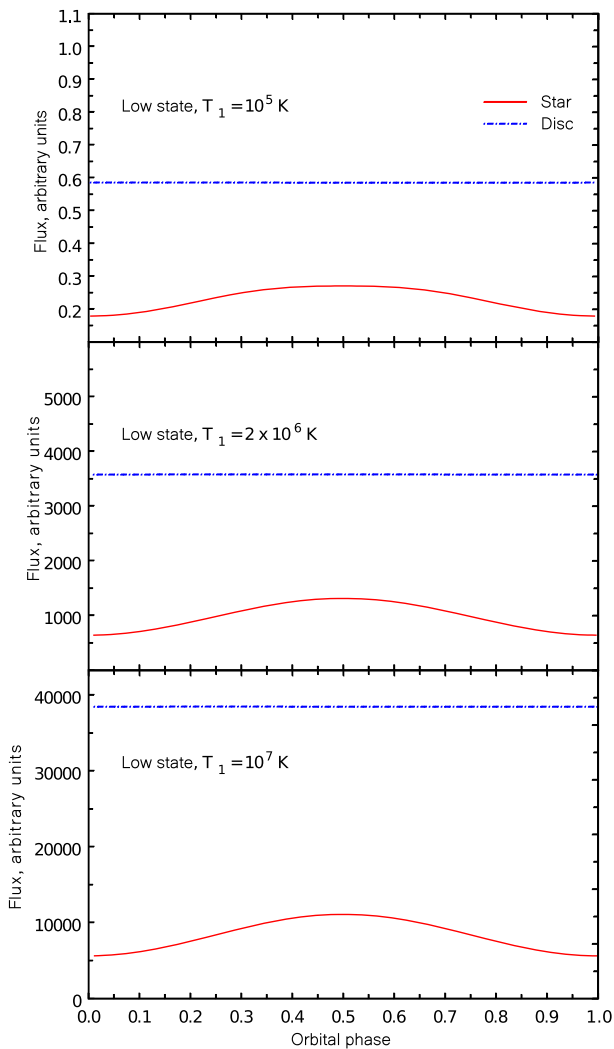


Figure 11. Light curves of the donor star and accretion disc computed as the inverse problem solution for the low state, $T_1 = 10^5$, 2×10^6 , and 10^7 K. The results for the high state and average curve are qualitatively similar to these curves.

about 10 per cent of the X-ray flux that fell from its central part to its outer part was thermally converted to the optical range). It can be supposed that the other 90 per cent of falling flux was scattered by the outer layers of the disc without a significant change in the frequency or was converted to the energy of convective motion in the disc. We analysed the average light curve of Sco X-1 ($T_1 = 5 \times 10^5$ K) using the following values of parameters for the model: $\beta_d = 14^\circ$, $\eta_s = 0.5$, $\eta_d = 0.9$. The results of this analysis (dependences of residuals for parameters q , i) are shown in Fig. 14. It can be seen that the increase in the opening angle of the disc from 3.2 – 14° and the introduction of a non-zero albedo ($\eta_s = 0.5$, $\eta_d = 0.9$) led to a weak change in the mass ratio ($q = 3.6$) and to the value of the orbital inclination $i \approx 30^\circ$.

Table 6 contains the parameters of the Sco X-1 system that correspond to optimal values of q , i for different values of the disc opening angle β_d and albedos η_s , η_d . It can be seen that for every fixed pair of q , i the values of the parameters for the donor star and accretion disc were close to the parameters found above for the average light curve for $\beta_d = 3.2^\circ$ and $\eta_s = \eta_d = 0$ (see Table 2). The temperature of the non-disturbed star was $T_2 \approx 3000$ K, the average

temperature of the heated part of the star was 8000 – $11\,000$ K, the radius of the accretion disc $R_d = (0.362$ – $0.420)\xi$ was slightly less than in the case of $\beta_d = 3.2^\circ$, $\eta_s = \eta_d = 0$ ($R_d = 0.637\xi$), and the temperature of the outer part was higher ($32\,000$ – $52\,600$ K instead of $11\,500$ K) because of the smaller radius and higher β_d .

The optical luminosity of the accretion disc dominated in the total optical luminosity of Sco X-1. The contribution of the optical star was $\lesssim 20$ per cent as seen earlier (see Fig. 7).

To find the physical characteristics of the system we accepted the following optimal values of parameters q , i (taking into account Tables 2 and 6): $q = 3.6$ (3.5 – 3.8), $i = 30^\circ$ (25 – 34°), where the brackets show the lower and upper limits of the parameters defined mostly by the uncertainty of the physical model of the Sco X-1 system rather than by errors of observations.

Fig. 15 shows theoretical light curves (in arbitrary units) of the donor star and accretion disc in the case of a non-zero X-ray albedo and thick accretion disc ($\eta_s = 0.5$, $\eta_d = 0.9$, $\beta_d = 14^\circ$).

6 DISCUSSION

Let us discuss the results obtained in Section 4 ($\beta_d = 3.2^\circ$, $\eta_s = \eta_d = 0$), where the inverse problem was investigated in a wide range of X-ray luminosity L_X . In the case of low orbital inclination ($i = 25$ – 20° , corresponding to the model in Section 4) the formation zone of Bowen lines should be close to the terminator of the heated star (where the temperature of the star’s photosphere is low), whereas for high values of the orbital inclination this zone should be close to the Lagrange point (where the temperature of the star’s photosphere is high); therefore we discuss here the case of low inclinations. The semi-amplitude of radial velocities of Sco X-1 obtained using narrow emission Bowen lines N III/C III was $K_v = 74.9$ km s $^{-1}$ (Galloway et al. 2014). The corresponding mass function of the optical star was $0.0343 M_\odot$, which leads to $M_x \geq 0.0569 M_\odot$ for $q = 3.5$. Since Bowen lines were formed on the heated (by X-rays) part of the optical star, the value of $K_v = 74.9$ km s $^{-1}$ was underestimated in comparison with the real K_v that corresponds to the star’s centre of masses. So, the mass function $f_v(M) = 0.0343 M_\odot$ was just a lower limit of the real mass function in the Sco X-1 system. In the model under discussion (with $\eta_s = \eta_d = 0$, $\beta_d = 3.2^\circ$) knowledge of the values of the inclination of the orbit $i = 25$ – 20° and of the mass ratio $q = M_x/M_v = 3.5$ allowed us to estimate the lower limit of the mass of the relativistic object M_x from the mass function $f_v(M) = 0.034 M_\odot$: $M_x \geq 0.75 M_\odot$ for $i = 25^\circ$ and $M_x \geq 1.42 M_\odot$ for $i = 20^\circ$. It is interesting to note that for $i = 20^\circ$ from our computed interval of i the corresponding lower limit of the mass of the relativistic object was close to the average mass of the neutron star $1.4 M_\odot$. If we assume this value of the relativistic object’s mass we should assume that the Bowen lines N III/C III were formed on the part of the photosphere of the optical star that was close to its centre of masses. This is physically unrealistic, because (as already mentioned) the temperature of the surface of the optical star around such a region (close to the terminator separating the heated and non-heated parts of the star) is too low (≈ 3000 K) to excite ions of N III/C III. However, because of the high X-ray heating even in the vicinity of the terminator, a zone with an inverse temperature distribution can form (like the solar chromosphere). In the upper layers of such a ‘chromosphere’, physical conditions can become favourable for the formation of Bowen lines.

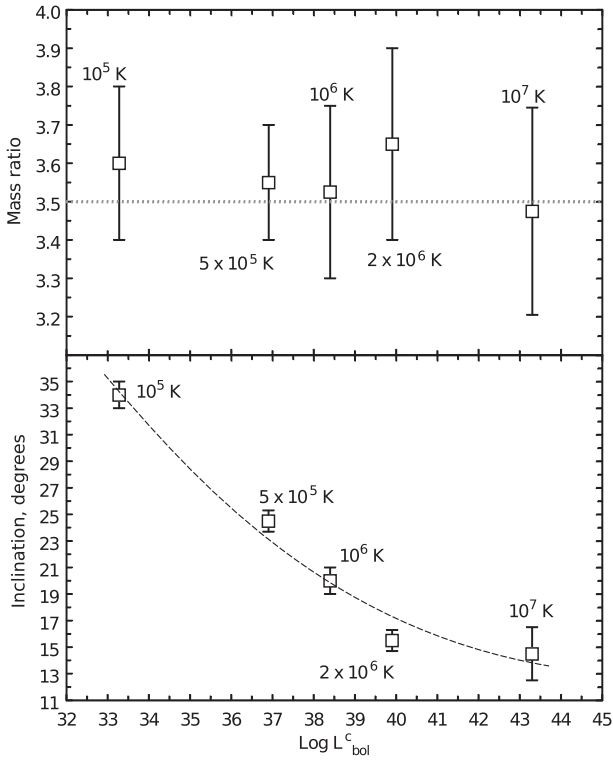
For the value $i = 25^\circ$ from our computed interval of i , the corresponding mass of the relativistic object $M_x = 0.75 M_\odot$, significantly lower than the neutron star’s mass $1.4 M_\odot$. In order to extract the mass of the relativistic object from spectral data for $i = 25^\circ$ that would

Table 5. Parameters of Sco X-1 for different values of T_1 (which characterizes the X-ray heating in the case of $\eta_s = \eta_d = 0$, $\beta_d = 3.2^\circ$).

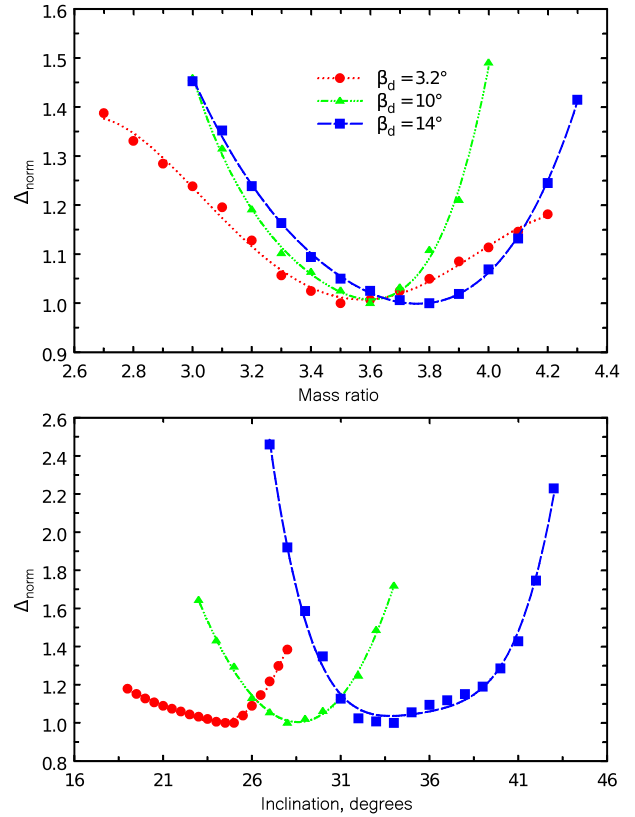
T_1 , K	R_1 , a_0	R_1 , cm	$L_{\text{bol}}^c = 4\pi\sigma T_{\text{in}}^4 R_1^2$, erg s $^{-1}$	i , °	$q = \frac{M_x}{M_v}$	M_x^* , M_\odot	\overline{K}_v^{**} , km s $^{-1}$
1×10^5	0.000 54	1.64×10^8	1.9×10^{33}	34	3.5	0.32	122
5×10^5	0.001 36	4.13×10^8	8.0×10^{36}	25	3.5	0.75	92.6
1×10^6	0.001 96	5.96×10^8	2.5×10^{38}	20	3.5	1.42	74.9
2×10^6	0.002 69	8.18×10^8	8.0×10^{39}	15.5	3.5	2.97	58.5
1×10^7	0.005 75	1.75×10^9	2.0×10^{43}	14.5	3.5	3.61	54.8

Notes.* M_x values were calculated using $K_v = 74.9 \text{ km s}^{-1}$ (i.e. $f_v(M) \approx 0.0343 M_\odot$).

**These values of \overline{K}_v are required for definite values of i under the assumption of the same value of the neutron star mass $M_x = 1.4 M_\odot$.


Figure 12. Dependence of q and i on the bolometric luminosity of the central part of the accretion disc in the low state (which characterizes the X-ray heating). The corresponding value of T_1 is indicated. In the range $L_{\text{bol}}^c = 3.3 \times 10^{36} - 2.6 \times 10^{38} \text{ erg s}^{-1}$ ($\log L_{\text{bol}}^c = 36.9 - 38.4$), close to observed values of the Sco X-1 luminosity) the inclination angle of the orbit was $i = 25 - 20^\circ$. The star fully filled its Roche lobe, $\eta_s = 0$, $\eta_d = 0$, $\beta_d = 3.2^\circ$.

be equal to the mass of the neutron star $1.4 M_\odot$ it was necessary to increase the observed semi-amplitude of radial velocities K_v from 74.9 to 92.9 km s^{-1} , i.e. by a factor of 1.24 . In this case the region of Bowen-line formation did not coincide with the optical star's centre of masses. The region was shifted from it in the direction of the relativistic object by $0.24a_v$, where a_v is the radius of the absolute orbit of the optical star. Since the absolute orbital radius a_v and the distance between centres of masses of components a_0 are connected by the relation $a_v = a_0 \frac{q}{1+q} \approx 0.78a_0$ the shift of the region of the Bowen-line origin from the centre of masses of the optical star was $\approx 0.19a_0$. The distance between the centre of the star's masses and the L1 point was $0.37a_0$. As can be seen from Figs 6(a)–(c), the


Figure 13. Dependences of relative residuals minimized over all parameters except the mass ratio q (upper panel) and inclination i (lower panel) for the average light curve and different values of the disc's opening angle, $\eta_d = 0$, $T_1 = 5 \times 10^5 \text{ K}$.

location of the region of Bowen-line formation on the heated part of the star's surface in this case corresponded to $j = 4 - 5$, where j is the number of cross-sections of the star's body counted from the Lagrange point L1. For $T_1 = 10^6 \text{ K}$ the temperature at this point (see Fig. 6c) in the high state was $\approx 48\,000 \text{ K}$; for $T_1 = 5 \times 10^5 \text{ K}$ it was $\approx 18\,000 \text{ K}$. The temperature in these regions on the heated part of the star significantly exceeded $10\,000 \text{ K}$, allowing the formation of Bowen N III/C III lines. It is possible to move the region of Bowen-line formation even further from the optical star's centre of masses (and, correspondingly, from the terminator) if we assume that the neutron star's mass in the Sco X-1 system exceeds the standard value $1.4 M_\odot$. So far, there have been found several binary systems with masses of pulsars (i.e. of neutron stars) close to $2 M_\odot$ (see e.g. Cherepashchuk 2013). If we assume that there is a massive neutron

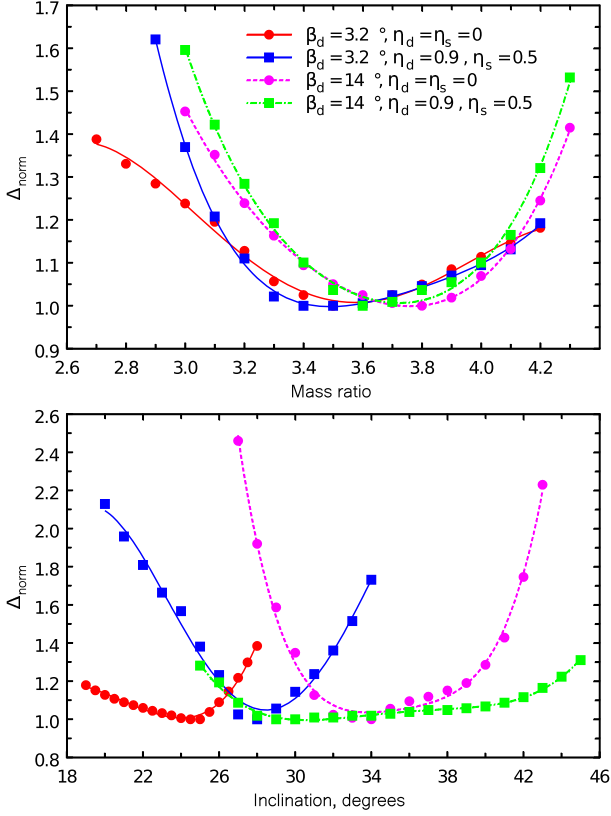


Figure 14. The same as Fig. 13 for the following values of the disc’s opening angle and X-ray albedo of the star and disc: $\beta_d = 3.2^\circ$, $\beta_d = 14^\circ$, $\eta_d = \eta_s = 0$, $\eta_s = 0.5$, and $\eta_d = 0.9$.

Table 6. Parameters of Sco X-1 for different values of β_d , η_s , and η_d , $T_1 = 500\,000$ K.

	$\eta_s = \eta_d = 0$		$\eta_s = 0.5, \eta_d = 0.9$
q	3.5	3.8	3.6
$i, ^\circ$	28	34	30
T_2, K	2950	2950	2950
$\langle T_{\text{warm}} \rangle, \text{K}$	8170	10930	8516
R_d, ξ	0.400	0.420	0.362
R_d, a_0	0.248	0.263	0.225
$\beta_d, ^\circ$	10	14	14
T_{in}, K	539300	682550	500930
T_{out}, K	52600	44860	31700
α_g, fixed	0.75	0.726	0.70
R_1, ξ	0.00200	0.00370	0.00362
R_1, a_0	0.00126	0.00234	0.00227
χ_{min}^2	146	126	103

star in the Sco X-1 system ($\approx 2 M_\odot$), it is necessary for $i = 25^\circ$ to increase the observed semi-amplitude of the radial velocities from 74.9 to 104.9 km s $^{-1}$, i.e. by a factor of 1.4. In this case the region of the origin of narrow emission Bowen lines N III/C III is shifted from the centre of the star’s masses towards the relativistic object by $0.4a_v = 0.31a_0$. This corresponds to $j = 1-2$ (see Figs 6a–c). The temperature here in the high state was $\approx 60\,000$ K for $T_1 = 10^6$ K and $\approx 25\,000$ K for $T_1 = 5 \times 10^5$ K. High values of the temperature of the heated part of the optical star are favourable for the formation of the Bowen lines N III/C III.

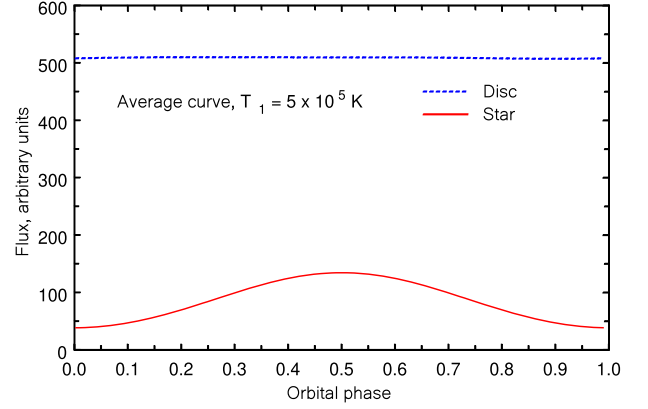


Figure 15. Light curves of the donor star and accretion disc computed as the inverse problem solution for the average light curve, $\eta_s = 0.5$, $\eta_d = 0.9$, $\beta_d = 14^\circ$.

For the inclination $i = 30^\circ$ (25–34 $^\circ$) the zone of formation of Bowen lines lies in the region with high temperatures of the photosphere of the heated optical star.

7 CONCLUSIONS

We have interpreted optical orbital light curves of the Sco X-1 system using a model of an interacting binary system with the donor star filling its Roche lobe and an accretion disc around the relativistic object (neutron star).

We investigated our inverse problem in a wide range of parameters. The luminosity of the X-ray source L_X was changed over a very wide range from 1.9×10^{33} – 2.0×10^{43} erg s $^{-1}$ (see Table 5). The disc opening angle (which characterizes the disc’s thickness and defines the size of the shadow on the donor star) was changed from $\beta_d = 3.2^\circ$ (the standard value in disc accretion theory, Shakura & Sunyaev 1973) to $\beta_d = 10, 14^\circ$. Cases of the X-ray albedo of the disc $\eta_d = 0$ and $\eta_d = 0.9$ were considered. The main conclusions of our paper are as follows:

(i) Calculations for the case $\beta_d = 3.2^\circ$, $\eta_s = 0$, $\eta_d = 0$, and the range of values of the X-ray luminosity $L_X = 1.9 \times 10^{33}$ – 2×10^{43} erg s $^{-1}$ showed that the mass ratio of components $q = M_x/M_v$ weakly depends on the value of L_X ; it was $q \approx 3.5$. The orbital inclination i significantly depends on the value of L_X and it decreased from $i = 34^\circ$ (for $L_X = 1.9 \times 10^{33}$ erg s $^{-1}$) to $i = 14.5^\circ$ (for $L_X = 2 \times 10^{43}$ erg s $^{-1}$). For the physically realistic value $L_X = 8 \times 10^{36}$ erg s $^{-1}$ the values of q and i were equal to 3.5 and 25° correspondingly.

(ii) The calculation for the case $\eta_s = \eta_d = 0$, $L_X = 8 \times 10^{36}$ for values of the accretion disc opening angle $\beta_d = 10, 14^\circ$ showed that an increase in this angle leads to a significant increase in the orbital inclination i and to a weak increase in the mass ratio q (see Table 6). For the value $\beta_d = 10^\circ$ the corresponding values were $q = 3.5$, $i = 28^\circ$; for the value $\beta_d = 14^\circ$ they were $q = 3.8$ and $i = 34^\circ$.

(iii) The calculation for $L_X = 8 \times 10^{36}$ erg s $^{-1}$ and for values $\beta_d = 14^\circ$, $\eta_s = 0.5$, $\eta_d = 0.9$ gave the following results: $q = 3.6$, $i = 30^\circ$. Finally, we chose the following optimal values of parameters q, i : $q \approx 3.6$ (3.5–3.8), $i = 30^\circ$ (25–34 $^\circ$), where in the brackets we show the lower and upper limits of q, i that were mostly defined by the uncertainty of the physical model of the Sco X-1 system.

(iv) From the observational lower limit of the mass function of the optical star $f_v(M) = 0.0343 M_\odot$ obtained from the semi-amplitude of the radial velocity for narrow Bowen lines $K_v = 74.9$ km s $^{-1}$ for

$q = 3.6$, $i = 30^\circ$, the estimates of masses of the relativistic object and optical star were $M_x > 0.45 M_\odot$, $M_v > 0.12 M_\odot$ correspondingly. To get the mass of the neutron star $M_x = 1.4 M_\odot$ it was necessary to increase the semi-amplitude of the radial velocity of the optical star from $K_v = 74.9$ to $\approx 110 \text{ km s}^{-1}$, i.e. by 1.47 times. This indicates that the zone of formation of narrow emission Bowen lines in the Sco X-1 system was displaced from the centre of mass of the optical star toward the Lagrange point L1 by the value $0.44 a_v$, where a_v is the radius of the absolute orbit of the optical star. In this region the temperature of the heated part of the optical star was significantly greater than 10 000 K, which is favourable for the formation of emission lines N III/C III. In addition, the temperature of the wind that moves from the star's heated part can be higher than on the photosphere level, and this fact is also favourable for the formation of Bowen lines.

(v) For the value $q = 3.6$ and for the neutron star's mass $1.4 M_\odot$ the possible mass of the optical star is $M_v \approx 0.4 M_\odot$. The temperature of the non-heated optical star $T_2 \approx 3000 \text{ K}$, corresponding to the spectral type M4–M5V. The average radius of the optical star R_2 that filled its Roche lobe was $\approx 1.25 R_\odot$. The bolometric luminosity of the star was $L_{\text{bol}} = 4\pi R_2^2 \sigma T_2^4 = (2.1\text{--}4.6) \times 10^{32} \text{ erg s}^{-1}$. So, the optical star in the Sco X-1 system possessed significant excesses of radius and luminosity, i.e. it moves in its evolutionary way and has undergone a significant mass-loss. Its initial mass should be greater than $0.8 M_\odot$. The mass of the donor star was probably reduced due to the mass-loss from the system in the stellar wind that was induced by the strong X-ray heating (Basko & Sunyaev 1973; Iben et al. 1995). Another possibility consists in that the star is not in thermal equilibrium and has a radius excess according to its mass due to the rapid mass-loss.

(vi) The amplitude of the 'reflection effect' for the donor star only (after subtraction of the accretion disc's radiation) is maximal in the high state and decreases during the transition to the low state (and is lower for the average light curve). Since the isolated star cannot sufficiently change its surface temperature distribution with time to explain the amplitude of the light curve, we have strong reasons to claim that the main cause of the transition of Sco X-1 from the high state to the low state is the variability of the X-ray flux from the accreting neutron star. Under the assumption that the main cause of the change in the X-ray flux falling on the donor star is the change in the temperature in our modelling, the X-ray flux dropped by a factor of 3.3 (for $T_1 = 10^6 \text{ K}$) and by a factor of 2.4 (for $T_1 = 5 \times 10^5 \text{ K}$) during the transition between high and low states. It is essential to note that this result is related to the variability of Sco X-1 on long time-scales. On short time-scales the correlation between the X-ray and optical fluxes in the system is more complicated (Hynes et al. 2016): in the high state optical fluxes are correlated with X-ray fluxes; in the low state they are anticorrelated.

(vii) The optical luminosity of the accretion disc dominates in the total optical emission of Sco X-1 and is greater than the average luminosity of the donor star by a factor of 4–8. This explains the invisibility of absorption lines of the donor star in the system's spectrum and the relative weakness of narrow Bowen emission lines (Galloway et al. 2014). The optical luminosity of the accretion disc, along with the amplitude of the 'reflection effect', drops during the transition from the high state to the low state; we explain this drop with the variability of the X-ray flux from the central source (Shakura & Sunyaev 1973).

(viii) Our calculations showed that during the transition of Sco X-1 from the high state to the low state the total optical flux from the system dropped by ≈ 35 per cent. The drop of the average flux

from the donor star was ≈ 5 per cent, and it was ≈ 30 per cent for the accretion disc's flux. Contributions from the hot line and the hotspot were negligible (≈ 1 per cent of the total flux in the high state, ≈ 4 per cent in the low state).

(ix) The ratio between optical fluxes of the accretion disc and of the donor star remained unchanged during the transition from the high state to the low state in a wide range of q and i parameters changes; i.e. our conclusion about the domination of the optical emission of the accretion disc in the total optical emission of Sco X-1 is reliable.

The question about the nature of the bimodal behaviour of the Sco X-1 system (the presence of low and high states in the optical light curve differing by 0.4 mag) is a separate problem that was outside the scope of this study. We make only several brief notes.

Slow changes in the average brightness combined with orbital variability have been observed in different types of binary systems. For example, in X-ray binaries with black holes in quiescence (when the X-ray luminosity is negligible) there have been observed transitions from the passive state to the active state. During this process the average brightness of the system increases by several tenths of the stellar magnitude (Cantrell et al. 2008, 2010; Cherepashchuk et al. 2019a, b). In the A0620–00 system the transition from the passive to the active state is accompanied by the start of strong irregular variability in the brightness (flickering); in the system XTEJ1118+480 the growth of the average system's brightness is not accompanied by flickering (Cherepashchuk et al. 2019a, b). Cherepashchuk et al. (2019a) suggested a hypothesis that the transition of an X-ray nova from the passive state to the active state and vice versa can be connected with movements of active regions of the donor star through the Lagrange point L1. Since the mass transfer rate through the L1 point strongly (as $(\Delta R/R)^3$) depends on the degree of Roche-lobe overflow ΔR (Paczynski & Sienkiewicz 1972) such movements can lead to significant changes in the rate of matter consumption by the accretion disc and then to slow changes in the optical brightness of accretion structures.

In the case of Sco X-1 such a mechanism has low probability, because the influence of active regions on the donor star is suppressed by the strong X-ray heating. It seems that effects arising from the variability of the X-ray heating (influencing the rate of mass transfer through the L1 point) and from the interaction between winds from the star and disc (winds are induced by strong X-ray heating, Basko & Sunyaev 1973) are important. The effects of eclipses of the central X-ray source by gas streams and structures in the accretion disc could also be important, because they can lead to a decrease in the X-ray flux falling on an optical star even if the luminosity of the X-ray source is constant. Therefore, three-dimensional gas-dynamical calculations of such processes in binary X-ray systems are very important.

ACKNOWLEDGEMENTS

The work was supported by the Russian Science Foundation grant 17-12-01241 and by the Scientific and Educational School of M. V. Lomonosov Moscow State University 'Fundamental and applied space research' (AMC). The authors acknowledge support from the M. V. Lomonosov Moscow State University Program of Development.

We are grateful to the anonymous referee for their valuable comments that helped to significantly improve the quality of the paper.

DATA AVAILABILITY

The data underlying this article will be shared on reasonable request to the corresponding author.

REFERENCES

- Antokhina E. A., Cherepashchuk A. M., Shimanskii V. V., 2005, *Astron. Rep.*, 49, 109
- Augusteijn T. et al., 1992, *A&A*, 265, 177
- Basko M. M., Sunyaev R. A., 1973, *Ap&SS*, 23, 117
- Bisikalo D. V., 2005, *Ap&SS*, 296, 391
- Bisnovatyi-Kogan G. S., Blinnikov S. I., 1977, *A&A*, 59, 111
- Bradt H. V. et al., 1975, *ApJ*, 197, 443
- Britt C. T., 2013, PhD thesis, Louisiana State Univ.
- Canizares C. R. et al., 1975, *ApJ*, 197, 457
- Cantrell A. G., Bailyn C. D., McClintock J. E., Orosz J. A., 2008, *ApJ*, 673, L159
- Cantrell A. G. et al., 2010, *ApJ*, 710, 1127
- Cherepashchuk A. M., 2013, *Close Binary Stars*. Fizmatlit, Moscow [in Russian]
- Cherepashchuk A. M., Efremov Y. N., Kurochkin N. E., Shakura N. I., Sunyaev R. A., 1972, *Inf. Bull. Var. Stars*, 720, 1
- Cherepashchuk A. M., Katysheva N. A., Khruzina T. S., Shugarov S. Y., 1996, *Highly Evolved Close Binary Stars*. Gordon and Breach, Amsterdam
- Cherepashchuk A. M., Katysheva N. A., Khruzina T. S., Shugarov S. Y., Tatarskiy A. M., Burlak M. A., Shatsky N. I., 2019a, *MNRAS*, 483, 1067
- Cherepashchuk A. M., Katysheva N. A., Khruzina T. S., Shugarov S. Y., Tatarskiy A. M., Bogomazov A. I., 2019b, *MNRAS*, 490, 3287
- Church M. J., Gibiec A., Bałucińska-Church M., Jackson N. K., 2012, *A&A*, 546, A35
- Cowley A. P., Crampton D., 1975, *ApJ*, 201, L65
- de Jong J. A., van Paradijs J., Augusteijn T., 1996, *A&A*, 314, 484
- Dubus G., Lasota J.-P., Hameury J.-M., Charles P., 1999, *MNRAS*, 303, 139
- Galloway D. K., Premachandra S., Steeghs D., Marsh T., Casares J., Cornelisse R., 2014, *ApJ*, 781, 14
- Giacconi R., Gursky H., Paolini F. R., Rossi B. B., 1962, *Phys. Rev. Lett.*, 9, 439
- Gottlieb E. W., Wright E. L., Liller W., 1975, *ApJ*, 195, L33
- Habets G. M. H. J., Heintze J. R. W., 1981, *A&AS*, 46, 193
- Hakala P., Ramsay G., Barclay T., Charles P., 2015, *MNRAS*, 453, L6
- Hasinger G., van der Klis M., 1989, *A&A*, 225, 79
- Hiltner W. A., Mook D. E., 1967, *ApJ*, 150, 851
- Hiltner W. A., Mook D. E., 1970, *A&A*, 8, 1
- Himmelblau D. M., 1972, *Applied Nonlinear Programming*. McGraw-Hill, New York
- Hynes R. I., Schaefer B. E., Baum Z. A., Hsu C.-C., Cherry M. L., Scaringi S., 2016, *MNRAS*, 459, 3596
- Iben I., Jr, Tutukov A. V., Yungelson L. R., 1995, *ApJS*, 100, 233
- Ilovaisky S. A., Chevalier C., White N. E., Mason K. O., Sanford P. W., Delvaile J. P., Schnopper H. W., 1980, *MNRAS*, 191, 81
- Khruzina T. S., 2011, *Astron. Rep.*, 55, 425
- Khruzina T. S., Cherepashchuk A. M., Bisikalo D. V., Boyarchuk A. A., Kuznetsov O. A., 2001, *Astron. Rep.*, 45, 538
- Khruzina T. S., Cherepashchuk A. M., Bisikalo D. V., Boyarchuk A. A., Kuznetsov O. A., 2003a, *Astron. Rep.*, 47, 214
- Khruzina T. S., Cherepashchuk A. M., Bisikalo D. V., Boyarchuk A. A., Kuznetsov O. A., 2003b, *Astron. Rep.*, 47, 848
- Khruzina T. S., Cherepashchuk A. M., Bisikalo D. V., Boyarchuk A. A., Kuznetsov O. A., 2005, *Astron. Rep.*, 49, 79
- Khruzina T. S., Golysheva P. Y., Katysheva N. A., Shugarov S. Y., Shakura N. I., 2015, *Astron. Rep.*, 59, 288
- Knigge C., 2006, *MNRAS*, 373, 484
- Lucy L. B., 1967, *Z. Astrophys.*, 65, 89
- Lukin V. V., Malanchev K. L., Shakura N. I., Postnov K. A., Chechetkin V. M., Utrobin V. P., 2017, *MNRAS*, 467, 2934
- Lyutyi V. M., Syunyaev R. A., Cherepashchuk A. M., 1973, *SvA*, 17, 1
- Maloney P. R., Begelman M. C., 1997, *ApJ*, 491, L43
- Maloney P. R., Begelman M. C., Pringle J. E., 1996, *ApJ*, 472, 582
- McGowan K. E., Charles P. A., O'Donoghue D., Smale A. P., 2003, *MNRAS*, 345, 1039
- McNamara B. J. et al., 2003, *AJ*, 125, 1437
- Meyer F., Meyer-Hofmeister E., 1984, *A&A*, 132, 143
- Mitsuda K. et al., 1984, *PASJ*, 36, 741
- Mook D. E. et al., 1975, *ApJ*, 197, 425
- Muñoz-Darias T., Casares J., Martínez-Pais I. G., 2005, *ApJ*, 635, 502
- Muñoz-Darias T., Martínez-Pais I. G., Casares J., Dhillion V. S., Marsh T. R., Cornelisse R., Steeghs D., Charles P. A., 2007, *MNRAS*, 379, 1637
- Paczyński B., Sienkiewicz R., 1972, *Acta Astron.*, 22, 73
- Petro L. D., Bradt H. V., Kelley R. L., Horne K., Gomer R., 1981, *ApJ*, 251, L7
- Pringle J. E., 1996, *MNRAS*, 281, 357
- Sandage A. et al., 1966, *ApJ*, 146, 316
- Scaringi S., Maccarone T. J., Hynes R. I., Körding E., Ponti G., Knigge C., Britt C. T., van Winckel H., 2015, *MNRAS*, 451, 3857
- Shakura N. I., Sunyaev R. A., 1973, *A&A*, 500, 33
- Shklovskii I. S., 1968, *SvA*, 11, 749
- Vrtilek S. D., Penninx W., Raymond J. C., Verbunt F., Hertz P., Wood K., Lewin W. H. G., Mitsuda K., 1991, *ApJ*, 376, 278
- White N. E., Peacock A., Taylor B. G., 1985, *ApJ*, 296, 475
- Wilson R. E., Devinney E. J., 1971, *ApJ*, 166, 605

This paper has been typeset from a \LaTeX file prepared by the author.